6.4 GETTING RID OF EL NINO

Cécile Penland and Ludmila Matrosova
NOAA-CIRES/Climate Diagnostics Center
Boulder, CO 80305-3328

The effect of El Niño on atmospheric processes is best investigated in models where one has the ability to specify sea surface temperatures with and without the El Niño signal. Unfortunately, it has been difficult to eliminate the ENSO signal from historical data sets without eliminating the signal in the entire interannual frequency band, whether or not all of that signal is associated with El Niño. We present a method, based on the statistics of tropical IndoPacific sea surface temperature data, for identifying and removing most of the evolving El Niño signal while retaining the broadband frequency signal not associated with ENSO. We identify a large-scale trend pattern in the residual SSTs and also show evidence supporting the hypothesis that a tropical Atlantic SST dipole would be more consistently seen if El Niño did not mast the northern branch.

1. INTRODUCTION

It is sometimes desirable in numerical studies of El Niño's effects to specify sea surface temperatures (SSTs) from which the historical ENSO signal has been removed. Two possible ways of doing this come immediately to mind: one may filter the SSTs so as to isolate the frequency spectrum dominated by El Niño, the 2-7 year band, say, or one may regress the SSTs onto some index of El Niño and consider the residual. There are objections to both possibilities. In the frequency filter method, the definition of El Niño essentially includes all physical mechanisms making any contribution whatsoever to the defining frequency band. In the regression-residual method, one isolates only those ENSO signals contemporaneous with the chosen index, thus missing any delayed response.

2. THE FILTER

There is an alternate method based on the results of Penland and Sardeshmukh (1995), who found that the evolution tropical sea surface temperature (SST) anomalies could in large part be represented as a stable linear process maintained by stochastic forcing:

$$\frac{d\boldsymbol{x}}{dt} = \mathbf{B}\boldsymbol{x} + \boldsymbol{\xi}\,, \qquad (1)$$

where x_i is the sea surface temperature anomaly at location i, and ξ_i is the contribution to the dynamics from the stochastic forcing at location i. In this scenario, the linear operator **B** in the dynamical equation is non-normal, allowing transient growth of SST variance (e.g., Farrell 1988). That is, when the SST anomaly field projects strongly onto an optimal initial structure (Fig. 1a), the nonorthogonal eigenvectors of **B** evolve at different rates and interfere in such a way that the spatial variance of the anomaly field temporarily increases to a maximum (Fig. 1b).

In a procedure analogous to Penland and Sardeshmukh (1995), we consider COADS monthly SST data (Woodruff 2001). This time, we use data in the entire tropical strip between 30°N and 30°S. The data were consolidated onto a $4^o \times 10^o$ grid and subjected to a three-month running mean. The 1950-2000 climatology was then removed from the SST data and the anomalies were projected onto 20 Empirical Orthogonal Functions (EOFs) containing about two-thirds of the variance. Assuming that the SST anomalies obey dynamics described by Eq. (1), the matrix **B**, its normal modes, and the singular vectors of the propagator $exp(\mathbf{B}\tau)$ were estimated using Linear Inverse Modeling (LIM). We note that LIM is closely related to Principal Oscillation Pattern (POP) analysis (Von Storch et al. 1988); indeed, POP analysis is the first step of LIM.

The leading right and left singular vectors of the propagator at lead times τ between seven and nine months were found to be essentially indistinguishable. These singular vectors are, in fact, the optimal structure and ENSO mature pattern shown in Fig. 1. Now, it may appear that projecting onto one or the other of these patterns might be a good way to isolate the ENSO signal, but the same objection to the regression-residual method applies to that idea since each pattern in Fig. 1 is orthogonal to the rest of the SST anomaly field and, so, cannot by itself describe an evolving field.

The quandary is resolved by noting that linear combinations of three empirically derived, complex normal mode pairs dominate both patterns; the real part of each of these mode pairs is extremely similar to Fig. 1b, and the corresponding adjoints project strongly onto Fig. 1a (Fig. 2). These normal mode pairs, in fact, account for most of the

**Corresponding author address:* Cécile Penland, NOAA-CIRES/Climate Diagnostics Center, R/CDC1, 325 Broadway, Boulder, CO 80305-3328; e-mail: Cecile.Penland@noaa.gov.

development of a mature El Niño or La Niña pattern and have (decay times, periods) of (16 mo, 233 mo), (15 mo, 56 mo) and (7 mo, 25 mo). Thus, the linearly predictable ENSO signal can be removed from SST anomaly data by projecting the anomaly map at any time onto the adjoints of the relevant normal modes, and then subtracting out the normal mode patterns weighted by that date's projection.

a)

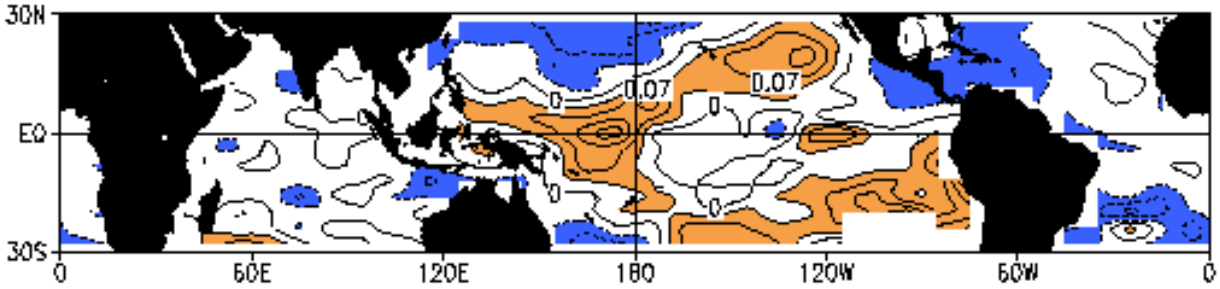

b)

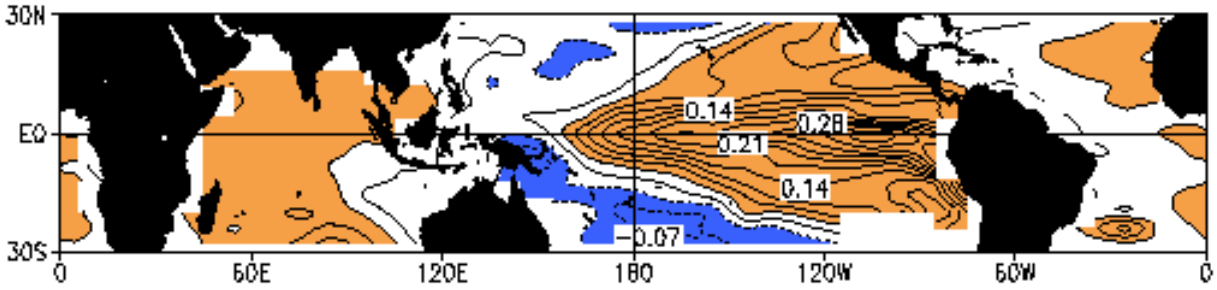

Fig. 1: a) Optimal initial pattern for growth. When the tropical SST anomaly field has a strong positive projection onto this pattern, a mature El Niño (Fig. 1b) is predicted to appear seven to nine months later. A strong negative projection implies evolution into La Niña. The field in Fig. 1a has been normalized to unity; the field variance in Fig. 2a is a factor of three to five larger.

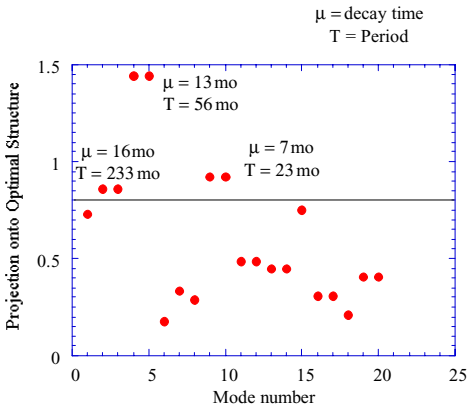

Fig. 2: Magnitude of the projection of empirically derived modal adjoints onto the optimal structure shown in Fig. 1a. Modes are numbered in order of decreasing decay time. Horizontal line is at 0.8.

3. RESULTS

This procedure was applied to the tropical SST data prepared as described above, thus separating the data into a set, which we call the linear ENSO signal, and another set, which we here call the background-pass filtered set. Spectra of the filtered and unfiltered SST data were evaluated at various locations throughout the tropics. Fig. 3 shows the time series of SST anomaly in the Niño 3.4 region (6°N – 6°S, 170°W – 120°W) before and after applying the background-pass filter.

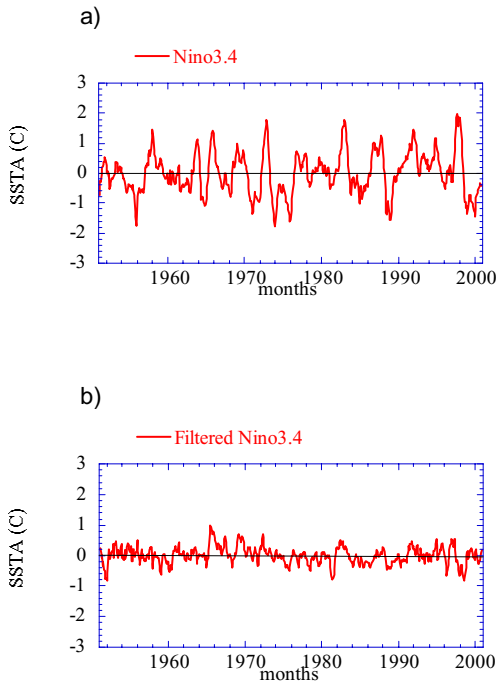

Fig.3: Time series of SST anomaly in the Niño 3.4 region before (a) and after (b) applying the background-pass filter.

It is not visually obvious in Fig. 3, but the filtered Niño 3.4 SST anomalies are dominated by low frequencies (Fig. 4). The efficiency of the filter in removing the broadband ENSO signal is displayed in Fig. 5.

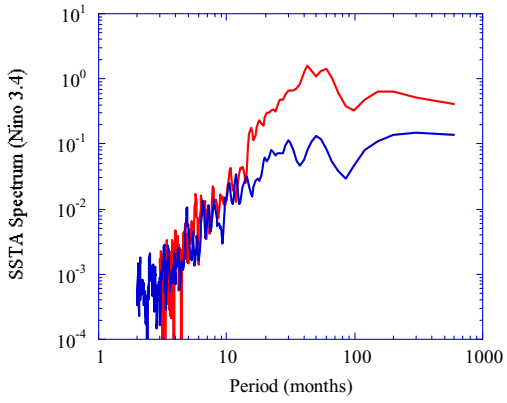

Fig. 4: FFT Spectrum of Niño 3.4 SST anomalies before (red) and after (blue) background-pass filtering.

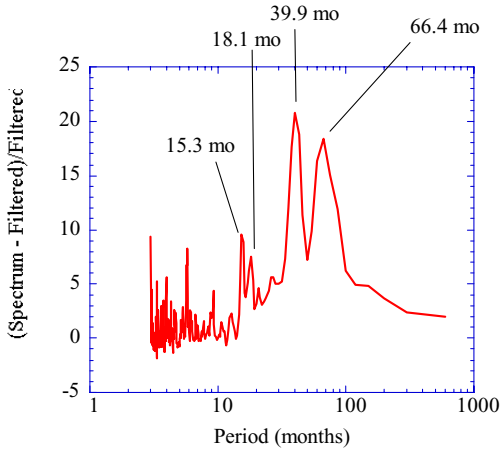

Fig. 5: Difference of spectra shown in Fig. 4, normalized to the background-pass filtered spectrum.

An advantage of this filter is that its application involves spatial patterns rather than long timeseries. Therefore, because the linear dynamics provides a unique correspondence between the spatial patterns and the frequencies associated with them, the filter can be applied at any temporal resolution. Further, it appears that the filter does not need to be recalculated for every data set; using the modes and adjoints evaluated from the COADS as described above when filtering weekly SST data since 1980 (Reynolds et al. 2002) was also successful (not shown).

To illustrate the advantage this method has over the regression-residual method of isolating the ENSO signal, we considered SST anomalies in the north tropical Atlantic Ocean. These anomalies have been shown by Enfield and Mayer (1997) and by Penland and Matrosova (1998) to be significantly correlated with SST anomalies in the east-central tropical Pacific at a lag of six months. In Figs. 6 and 7 we see that the residual formed by regressing north tropical Atlantic (NTA; see Penland and Matrosova 1998 for a definition) SST anomalies onto Niño 3.4 and then subtracting that signal from NTA SSTs has a spectrum practically indistinguishable from that of the original anomalies. In contrast, the modal filtering has indeed reduced spectral peaks associated with El Niño, although it is clear that the linear ENSO signal at interdecadal frequencies is stronger in NTA than the usual interannual frequencies associated with it. The spectra shown in Fig. 6 do suggest that some of the variance at frequencies usually associated with El Niño is not contained in the linear ENSO signal, although the significance of those peaks is debatable.

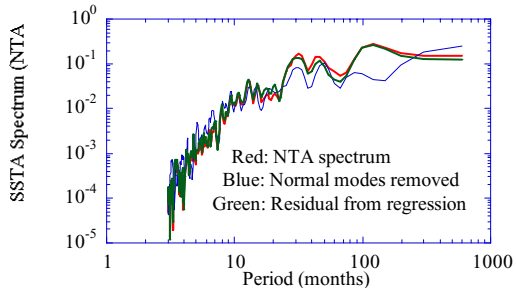

Fig. 6: As in Fig. 4, but for the NTA region. Also shown (green) is the FFT spectrum of the residual time series left when SST anomalies in NTA have been regressed onto those in the Niño 3.4 region and subtracted from the original NTA time series.

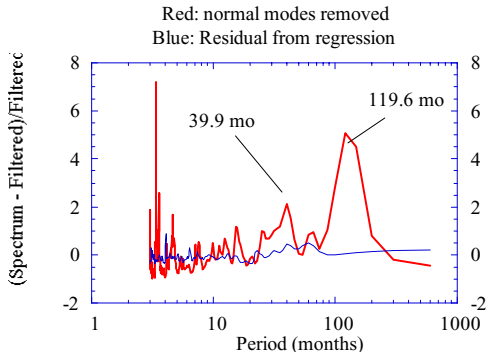

Fig. 7: As in Fig. 5, but for the NTA region. Blue line compares spectrum of regression-residual time series with that of original NTA SST anomalies.

In fact, it is interesting to compare the time series of NTA SSTA with and without the linear ENSO signal (Figs. 8 and 9). Fig. 8 shows a strong consistency with Figs. 6 and 7, with a striking change of character having occurred in the mid 1970's. This change is reminiscent of assertions (e.g., Graham 1995) that the climate suddenly shifted sometime around 1976.

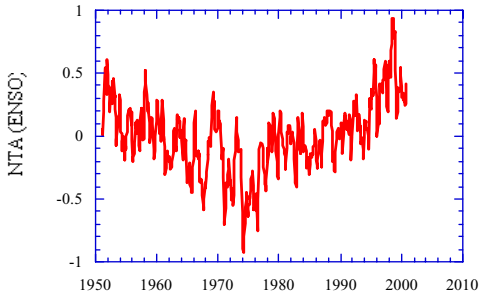

Fig. 8: Time series of NTA SST anomalies associated with the linear ENSO signal.

The curvature of these time series is interesting. In fact, particularly in the first part of the period, the background-pass NTA anomalies is affected by a global-scale trend pattern (i.e. EOF 1 after the modal filtering) whose variance is about half that of the ENSO pattern (i.e., EOF 1 *before* any modal filtering – not shown) in the entire tropical strip. This trend pattern is shown in Fig. 10, and its corresponding time series is shown in Fig. 11.

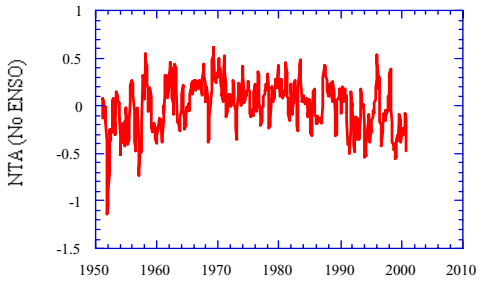

Fig. 9: Time series of background-pass filtered NTA SST anomalies.

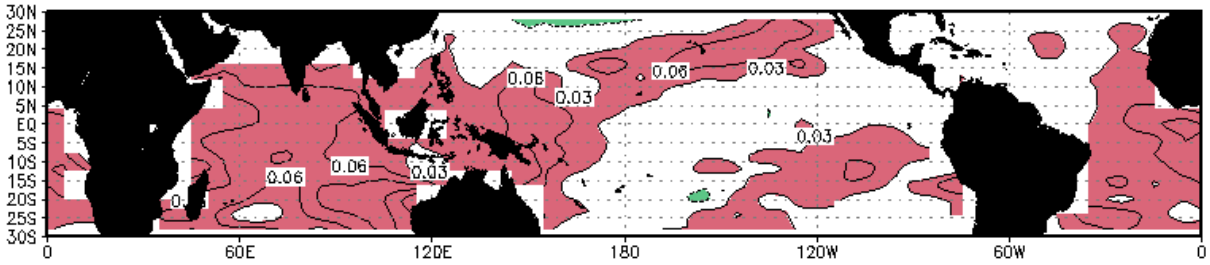

Fig. 10: First EOF of background-filtered SST anomaly. This pattern corresponds to an EOF eigenvalue of 13.3($^oC^2$), compared with the eigenvalue corresponding to the first EOF of the unfiltered SST anomaly, 29.8($^oC^2$).

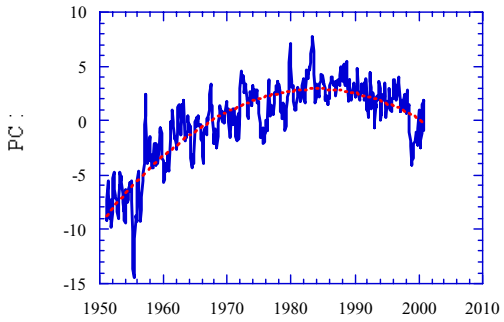

Fig. 11: Time series coefficient (solid blue line) of the pattern shown in Fig. 10. Dotted red line: quadratic fit to time series.

The trend pattern shown and its time series coefficient have several interesting properties. First, a quadratic fit to the time series shown in Fig. 11 explains more than 76% of the variance. Further, the trend pattern itself dominates the most persistent Principal Oscillation Pattern of the background-pass filtered SST, and does *not* contribute strongly to the others, suggesting that useful information about this pattern might be obtained from a univariate analysis. This is particularly true in the Indian Ocean. The background-pass filtered SST anomaly in a $4^o \times 20^o$ box centered on the equator at 80^o N is correlated with the trend timeseries at 0.90. Turning to the Atlantic, when quadratic fits to the filtered NTA and STA SST anomalies are removed from their time series, the residuals are signficantly anticorrelated at the 5% level. This supports the hypothesis suggested by Penland and Matrosova (1998) that a physical mechanism for a tropical Atlantic dipole does exist in nature, but that this dipole is rarely seen because El Niño disrupts the northern branch. A modification is in order, however; the large-scale trend preferentially disrupts the southern branch, although the anticorrelation is still significant at the 15% level even without accounting for that disruption.

Acknowledgements: The authors acknowledge conversations with Prashant Sardeshmukh, Klaus Weickmann and Jeff Whitaker. This work was supported by CLIVAR's Office of Global Change.

4. REFERENCES

Enfield, D.B., and D. A. Mayer, 1997: Tropical Atlantic SST variability and its relation to El Niño-Southern Oscillation. *J. Geophys. Res.*, **102**, 929-945.

Farrell, B. 1988: Optimal excitation of neutral Rossby waves. *J. Atmos.Sci.*, **45**, 163-172.

Graham, N.E., Simulation of recent global temperature trends, *Science*, **267**, 666-671.

Penland, C., and L. Matrosova, 1998: Prediction of tropical Atlantic sea surface temperatures using Linear Inverse Modeling*, J. Climate*, **11**, 483-496.

Penland, C., and P.D. Sardeshmukh, 1995: The optimal growth of tropical sea surface temperatures. *J. Climate* **8**, 1999-2024.

Reynolds, R.W., N.A. Rayner, T.M. Smith, D.C. Stokes, and W. Wang, 2002: An improved in situ and satellite SST analysis for climate*, J. Climate*, **16**, 1609-1625.

Von Storch, H., T. Bruns, L. Fischer-Bruns, and K. Hasselmann 1988: Principal Oscillation Pattern analysis of the 30-60 day oscillation in a GCM equatorial troposphere. *J. Geophys. Res.*, **93**, 11021-11036.

Woodruff, S.D., 2001: COADS updates including newly digitized data and the blend with the UK Meteorological Office Marine Data Bank. *Proceedings of International Workshop on Preparation, Processing and Use of Historical Marine Meteorological Data*, Tokyo, Japan, 28-29 November 2000, Japan Meteorological Agency and the Ship & Ocean Foundation, 9-13.